Archives of Photogrammetry, Cartography and Remote Sensing, Vol. 22, 2011, pp. 401-410
ISSN 2083-2214

THE POTENTIAL OF FULL-WAVEFORM LIDAR IN MOBILE MAPPING APPLICATIONS

Charles K. Toth [1], Piroska Zaletnyik [2], Sandor Laky [3], Dorota Grejner-Brzezinska [4]

[1, 4] The Center for Mapping, The Ohio State University 470 Hitchcock Hall, 2070 Neil Avenue, Columbus, OH 43210
toth@cfm.ohio-state.edu, dorota@cfm.ohio-state.edu
[2, 3] Department of Geodesy and Surveying,
Budapest University of Technology and Economics
Muegyetem rkp. 3, Budapest, H-1111, Hungary
laky.sandor@freemail.hu, zaletnyikp@gmail.com

KEY WORDS: LiDAR, Full-waveform, Discrete return, Classification

ABSTRACT: Full Waveform LiDAR data have been available for many years, yet applications just recently started discovering its potential in airborne topographic surveying. Forestry and earth sciences applications have been traditionally using waveform processing for many years, but topographic mapping has just started exploring the benefits of waveform. The potential advantages are improved point cloud generation, better object surface characterization, and support for object classification. However, there are several implementations and performance issues, such as the availability of waveform processing tools and waveform compression methods that should be addressed before applications can take full advantage of the availability of waveform data. The paper provides an overview of the waveform application potential in both airborne and mobile LiDAR mapping applications.

1. INTRODUCTION

The availability and use of Full Waveform Digitization (FWD) have been steadily growing in airborne LiDAR applications (Shan and Toth, 2009). These developments are mainly driven by two factors. First, technological advancements have improved system performance to the point that data storage is hardly a consideration, and, consequently, waveform data is easily available. In addition, sensor electronics developments provide better digitization capabilities in terms of improved signal quantization, shorter sampling rate, and longer sample records. Second, from a theoretical perspective, the full LiDAR waveform contains more information than discrete returns, which typically represent a subset of the waveform signal. Thus, as applications are searching for additional information sources to improve the value of any LiDAR-derived product, waveform is an obvious choice. Following general trends that software developments are behind the hardware, the availability of waveform processing software at the moment is basically limited to viewing capabilities; though research is active in this field and there are already a few processing methods to mainly address the needs of forestry applications.
The main benefits of waveform data are that it can provide better description of the object space geometry, primarily the vertical structure, and can support classification, such as

land-cover mapping. This study reviews the basics of the LiDAR waveform technology and compares its capabilities with respect to airborne and mobile platforms.

2. FULL WAVEFORM DIGITIZATION

Mobile LiDAR mapping systems, both airborne and Mobile LiDAR, are based on combining highly accurate georeferencing technologies with powerful pulsed laser sensing. Since the laser pulse is generated from a single device, laser rangefinder, a mechanical scanning mechanism is required to create a scanning laser beam. Note, that in general, the platform motion provides the second scanning direction, so that an area under an airplane can be more or less evenly ranged, or a 360° FOV rotating scanner on the vehicle can map the whole corridor around the vehicle path. Ignoring these aspects, there is very little functional difference between the systems designed for the two platforms; in fact, some systems, such as the RIEGL LMS-Q240i, are widely used on both airborne and mobile vehicle platforms.

The detection of the backscattered return signal, the waveform, has been an essential component of LiDAR systems, as it forms the basis for the range measurement. Note, the waveform is as old as the LiDAR technology itself. However, the lack of adequate sensor electronics and computer hardware made the access to digitized waveform practically impossible or unaffordable for a long time. Early systems used a simple threshold only to detect the arrival of the return pulse. Significant technological developments were needed to provide the whole waveform, which is frequently called Full Waveform Digitization. Figure 1 shows the process of waveform digitization.

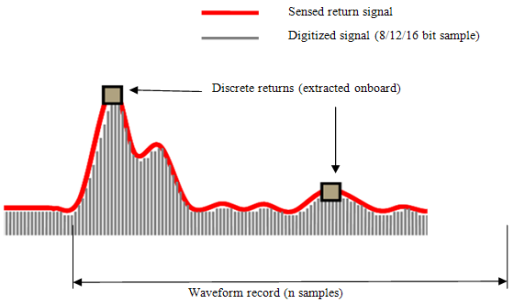

Fig. 1. Waveform digitization (Courtesy of Leica)

The effective length of the waveform depends a lot on the objects the reflection happens from, and systems have different solutions to make sure that only the significant part of the waveform is recorded. Obviously, a single return requires shorter sample length than a waveform generated by multiple returns from a tall tree. The two major solutions are the fixed length, where after detecting the presence of the waveform a certain number of samples are recorded, or variable length, where multiple sections of the waveform are recorded. In the latter case, when the waveform signal falls under the noise threshold, the digitization stops, and only resumes if the waveform signal is detected again (signal goes above the noise threshold). The typical sampling distance on modern systems is 1 ns, which translates to 15 cm distance (the measured range is half of the traveled distance by the laser pulse). The record length, the number of samples, generally falls in the range of 64-512.

Most systems offer a few options in terms of various record length and sampling rates to accommodate for different application requirements. Typical parameters including waveform digitizer capabilities are listed in Table 1 for broadly used systems.

Tab. 1. State-of-the-art airborne and mobile LiDAR systems

Airborne System	Mode	Scan Freq. [Hz]	Pulse Freq. [kHz]	Scanning Angle [°]	Beam Diverg. [mrad]	Pulse Energy [μJ]	Range Resolution [cm]	Pulse Length [ns]	Digitizer [ns]
Optech 2033	Oscillating	0-70	33	±20	0.2/1.0	N/A	1.0	8.0	N/A
Optech 3100	Oscillating	0-70	33-100	±25	0.3/0.8	<200	1.0	8.0	1
Optech Gemini	Oscillating	0-70	167	±25	0.15/0.25/0.8	<200	3.0	7.0	1
Optech Orion	Oscillating	0-100	167	±25	0.25	<200	2.0	7.0	N/A
Pegasus	Oscillating	0-140	400	±32.5	0.2	N/A	2.0	N/A	1
TopEye MkII	Conic	35	5-50	14,20	1.0	N/A	<1.0	4.0	0.5
TopoSys I	Line	653	83	±7.15	1.0	N/A	6.0	5.0	N/A
TopoSys II Falcon	Line	653	83	±7.15	1.0	N/A	2.0	5.0	1
Trimble Harrier	Rotating polygon	160	160	±30	0.5	N/A	2.0	4.0	1
Leica ALS50	Oscillating	25-70	83	±37.5	0.33	N/A	N/A	10	N/A
Leica ALS50-II	Oscillating	35-90	150	±37.5	0.22	N/A	N/A	10	1
Leica ALS60	Oscillating	0-100	200	±37.5	0.22	N/A	3.0-4.0	5.0	1
Riegl LMS-Q560	Line	160	240	±30.0	0.3	8	2.0	4.0	1
Riegl LMS-Q680i	Line	200	266	±30.0	0.5	8	2.0	4.0	1

Mobile LiDAR	Laser Units	Scan Freq. [Hz]	Pulse Freq. [kHz]	Scanning Angle [°]	Beam Diverg. [mrad]	Pulse Energy [μJ]	Range Resolution [cm]	Pulse Length [ns]	Digitizer [ns]
Optech Lynx	2	200	500	360	N/A	N/A	0.8	N/A	N/A
Riegl LMS-VQ250	2	200	600	360	0.3	N/A	0.5	N/A	N/A

3. FULL WAVEFORM PROCESSING

Since digitizing and storing waveforms are widely available by now, basic data acquisition technologies, the processing of waveforms is a user's choice; either to accept the real-time discrete return extraction offered by most manufacturers, or do the return extraction and additional waveform analysis in post-processing mode. Note that Riegl has many systems that only record the waveforms and no return extraction is done onboard; the discrete return extraction is only done in post-processing. There is no clear answer to which approach is better, as depending on the application specifics, both solutions, and even their combination, could be optimal. Table 2 list advantages and disadvantages of the two basic techniques. Note that the unnecessary separation of discrete return processing in real-time (online waveform processing) and return extraction in post-processing is more like an industry concept for marketing purposes.

Tab. 2. Discrete return vs. full waveform digitization

	Discrete Return	**Full Waveform Digitization**
Advantages	More manageable data volume Faster processing than FWD Many tools are available to process the data	Can provide much more detailed information about vertical elevation structure, surface slope and roughness Ability to distinguish an 'unlimited' number of targets in each waveform More flexibility and control in data processing and interpretation Possibility to define the way of calculating the range in post-processing potentially makes the ranging process more robust and accurate
Disadvantages	Coarse vertical resolution, discrete returns have to be separated by a few meters vertically (though, it is changing with shorter pulse length) Targets/objects separated by less than a meter vertically cannot be resolved by a discrete return system Pulse detection method applied depends on system manufacturer, user has no choice, while the method chosen can significantly affect accuracy	Data volume increases by a factor of 50-200 compared to discrete return systems Processing takes more time Not many tools are available to process full waveform data

4. RETURN/PULSE EXTRACTION METHODS

The techniques used to extract returns from waveforms have evolved over time as technology provided both better digitization and more computer power to process waveforms in either real-time or post-processing. Earlier techniques of detecting the arrival of the return pulse were based on using a simple threshold technique. Later, short-time

storage (buffering) of the return signal became available, and thus, provided a base for more complex methods for peak detection. For example, the center (gravity) of the return pulse shape or the Constant Fraction Discrimination (CFD) of the signal could be computed, and thus, better estimates became available. In addition, the detection of multiple peaks became feasible. Furthermore, various combinations of both hardware and software solutions resulted in techniques that are widely used in state-of-the-art LiDAR systems nowadays. Obviously, less, if anything, is known about the onboard methods, as manufacturers provide no information about their solutions for competitive reasons. Figure 2 shows two waveforms with peaks determined during the data acquisition (onboard), marked with x in magenta, clearly indicating that the peak extraction could not reach an optimal solution in these two cases. Figure 2a shows a waveform with two clearly visible peaks correctly detected, but there is an undetected third peak. Figure 2b depicts a situation where there are two peaks, and potentially a third and fourth one, which were jointly detected as a single peak. Note that these types of waveforms and peak extraction results are, in general, not typical.

Using simple widely available techniques, moving window with interval threshold and zero-crossing (first derivative), better return extraction can be achieved. The interval-based method (Billauer, 2008) correctly detects two peaks, marked in green, in both waveforms, but fails to extract the third peaks. The zero-crossing technique provides the best performance, as all the peaks, marked in red, are correctly detected in both waveforms. As an extension of the zero-crossing algorithm, the method described by (National Instruments, 2009) is based on the wavelet decomposition of the return signal and the detection of the zero crossings in the high level detail signal.

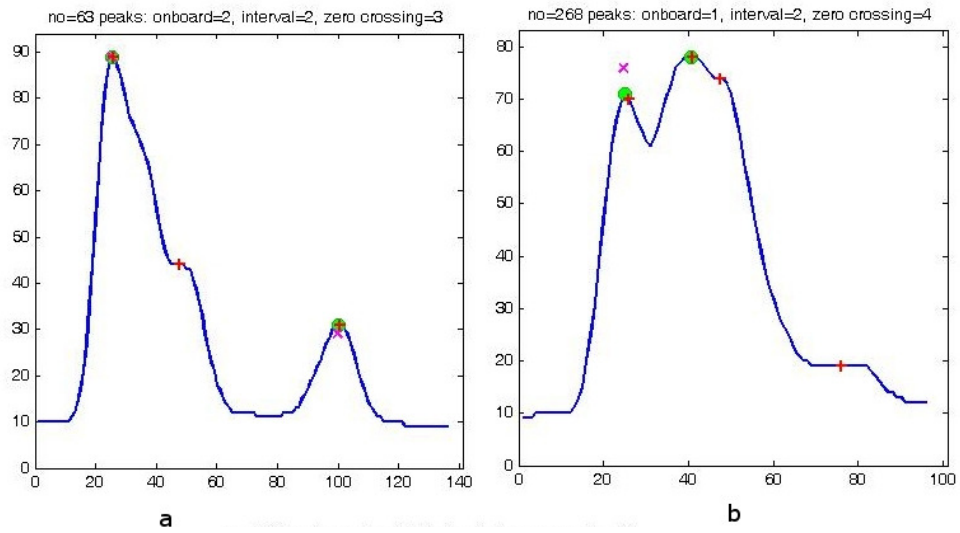

Fig. 2. Discrete returns extracted; x (magenta): onboard, circle (green) interval method, and + (red): zero-crossing technique

Another group of techniques is based on decomposing the waveform into the sum of components, or echoes (pulses/peaks), to generate a denser and more accurate 3D point cloud (Mallet and Bretar, 2009) by modeling the waveforms with Gaussian (Wagner *et al*., 2006), Generalized Gaussian or Lognormal functions (Chauve *et al*., 2007). Furthermore, the waveform decomposition into Gaussian components can be used not only for peak detection but can also discriminate between vegetation and non-vegetation points using the parameters of the Gaussian functions (Ducic *et al*., 2006), such as the amplitude and the standard deviation (pulse width). A similar approach (Mallet *et al*., 2008) used the Generalized Gaussian model for classifying urban areas with one more parameter, the shape parameter of the Generalized Gaussian model, which allows simulating Gaussian, flattened or peaked pulses, too. The Generalized Gaussian function is described in Eq. 1.

$$f_{GG,j}(x) = a_j \cdot \exp\left(-\frac{\left| x - \mu_j \right|^{\alpha_j^2}}{2\sigma_j^2} \right) \tag{1}$$

where, α=√2 is the Gaussian function, α=1 is the Laplacian function, and α>√2 represents a flattened Gaussian shape, μ and σ^2 stand for mean and variance, respectively.

The shape-based decomposition clearly provides a good performance for detecting multiple overlapping peaks. In addition, it offers valuable information (shape feature parameters) for classification. The high performance, however, comes at a price, as the method is iterative and takes a significant amount of computations; therefore, it is only available in post-processing. Note that good initial approximations, such as using onboard extracted peaks, can substantially reduce the processing time. Figure 3 illustrates two samples of waveform decomposition, including the residual functions. Figure 3a clearly indicates the high peak extraction capability of this method, as three highly-overlapping peaks are correctly detected. Figure 3b shows a more typical waveform, acquired over forested areas, with a large number of overlapping peaks.

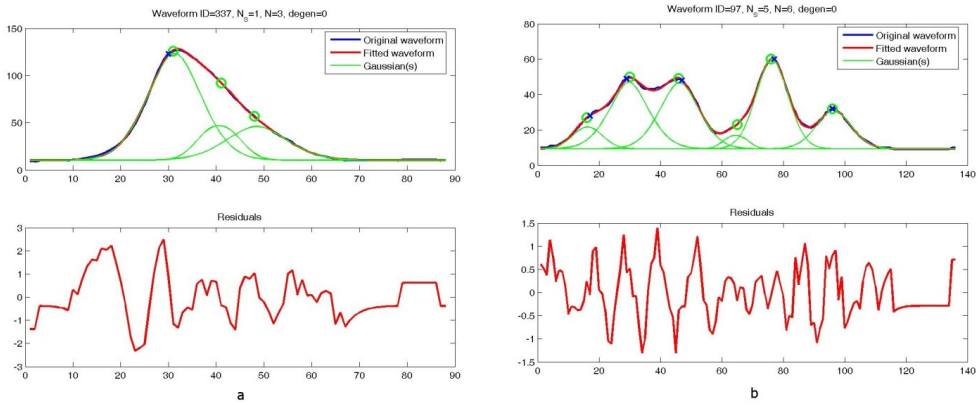

Fig. 3. Waveform decomposition-based peak extraction

To compare onboard discrete return extraction with methods available in post-processing, a comparative analysis based on a scan line, containing 1022 waveforms, extracted from a data set, acquired by an Optech 3100 Full-Waveform system, was performed. The selected area represented a mostly vegetated and suburban landscape in a region East of Dayton, Ohio. The waveforms were acquired at 70 kHz pulse rate, at 1 ns sampling with a maximum length of 440 samples (about 66 m in range) at an 8-bit intensity resolution (Optech, 2005). Table 3 and Figure 4 show the peak detection results as well as the computation time for the five tested methods.

Tab. 3. Peak detection performance results based on 1022 waveforms

Returns:	**1**	**2**	**3**	**4**	**5**	**6**	**7**	**8**	**9**	**Execution [s]**
Onboard	619	169	151	83	0	0	0	0	0	N/A
Threshold	645	185	150	33	9	0	0	0	0	0.50
Zerocrossing	627	179	133	55	25	2	0	1	0	0.22
Wavelet	624	187	114	54	32	10	0	0	1	5.20
Spline	390	350	150	74	38	14	3	1	2	32.07
Gaussian	306	306	167	141	72	23	6	0	1	1061.13

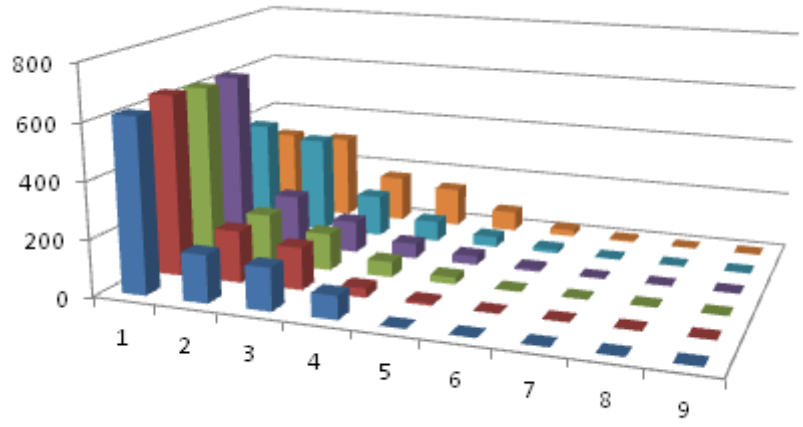

Fig. 4. Peak detection performance results based on 1022 waveforms (visualization of Table 3.)

The results in Table 3 confirm that, in general, more sophisticated methods can achieve higher peak detection performance. As expected, all five methods tested could extract more peaks in post-processing mode than the manufacturers provided real-time solution. In particular, the Gaussian function-based decomposition approach showed excellent performance for extracting highly-overlapping peaks, and thus detecting twice as many

peaks than the onboard solution in our tests. Since there was no absolute reference available for the waveforms, the results should be regarded as preliminary, although several randomly selected waveforms evaluated by an experienced operator indicated no misdetection.

Figure 4 is just the visualization of Table 3 to better illustrate that more complex processing results in a wider distribution of the detected multiple peaks in general.

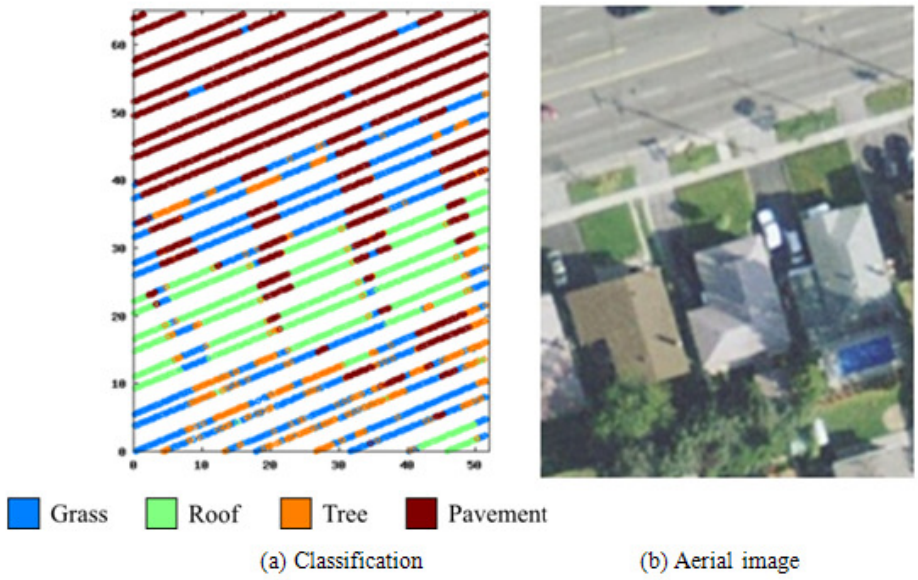

Fig. 5. Classification results

Tab. 4. Verification of the classification results

	Grass	**Roof**	**Tree**	**Pavement**
Grass	**21.6%**	0.0%	0.4%	0.7%
Roof	0.3%	**25.6%**	0.3%	0.1%
Tree	8.8%	0.4%	**4.2%**	0.0%
Pavement	1.9%	0.0%	2.2%	**33.5%**

5. CLASSIFICATION POTENTIAL OF WAVEFORM

ThBesides the benefit of better geometrical interpretation of the objects space, based on waveform data, the waveform may contain additional information that can be used to identify material or other characteristics of objects. An unsupervised classification method developed earlier (Laky *et al*., 2010a; Zaletnyik *et al*., 2010) was used to assess the land classification potential of the LiDAR waveform. This technique is based on statistical parameters of the echo waveforms, which provide the input to a Kohonen Self-Organizing Map (SOM) based neural network; the classifier output, in four classes, are combined with the discrete return data to obtain the final classification results. Figure 5 shows the results for 5934 waveforms acquired near Toronto, Canada, with reference image.

Visually comparing the results with an aerial imagery, the method, based on statistical parameters with unsupervised classification, classified the waveforms fairly effectively. For numerical validation, shown in Table 4, 700 sample points were manually classified using the aerial image. The rows are the classes of the manual classification, and the columns are the classes of the SOM-based classification. The percentages in the diagonal show the percentages of the waveforms that were correctly classified (84.9% of the waveforms). The most significant case of misclassification is 8.8% of the waveforms, which was manually classified as trees, but was classified as grass in the SOM-based approach. This possibly relates to seasonal changes.

6. CONCLUSION

The better exploitation of LiDAR waveform for topographic mapping was investigated in this study. The results, obtained by comparing pulses detected by discrete return systems during the data acquisition to various methods available in post-processing, indicated that the performance of the onboard return extraction can be improved. Obviously, this only applies to areas where more vertical resolution is needed to describe the objects, such as vegetated and urban areas; clearly, for open flat areas with hard surfaces, the geometrical description by discrete returns cannot be further improved. Most importantly, all post-processing methods can deliver nearly unlimited returns. In particular, the shaped-based method can robustly handle highly-overlapped peaks, though they may create ghost returns and require significantly more computation time.

The investigation on the feasibility of extracting information from waveform to support land cover classification produced encouraging results for a data set of about 6000 waveforms acquired over a residential area. Compared to a visual evaluation of about 10% of the waveforms, an 85% classification performance was achieved. The unsupervised classification results were combined with discrete returns to obtain the final classification. Based on the finding of this limited experience, it is expected that a similar performance could be achieved for more complex scenes, provided the classifier is better trained and the shape parameterization of the extracted peaks is also included in the process.

Comparing the waveform potential with respect to the two platforms, there are noticeable differences. First of all, the footprint is significantly different, and thus, on an average the complexity of waveforms obtained by Mobile LiDAR is below the airborne case; with respect to Mobile LiDAR, the airborne LiDAR appears as a large-footprint sensor. Therefore, it is likely that the classification potential of Mobile LiDAR is below that of the airborne case. Note, the shaped-based classification potential is much better for Mobile LiDAR, but that is based on the denser point cloud. Since the Mobile LiDAR has rather a small footprint, the surface orientation within the footprint is likely to be more homogenous than is the case for the airborne footprints. Therefore, the shape distortion due to incidence angles can be better preserved in the waveform, which could be only one pulse, and thus could be used for better object space reconstruction and interpretation.

ACKNOWLEDGEMENTS

The authors thank Optech International and Woolpert, Inc. for providing the data for this research. The third author is with the HAS-BME Research Group for Physical Geodesy and

Geodynamics at the Budapest University of Technology and Economics, Department of Geodesy and Surveying.

REFERENCES:

Billauer, E. (2008): Peakdet: Peak detection using MATLAB.
http://www.billauer.co.il/peakdet.html

Chauve, A., Mallet, C., Bretar, F., Durrieu, S., Pierrot-Deseilligny, M., Puech, W., 2007. Processing full-waveform LiDAR data: Modelling raw signals. *International Archives of Photogrammetry, Remote Sensing and Spatial Information Sciences* 36 (Part 3/W52), pp. 102-107.

Ducic, V., Hollaus, M., Ullrich, A., Wagner, W., Melzer, T., 2006. 3D vegetation mapping and classification using full-waveform laser scanning. In: Proc. Workshop on 3D Remote Sensing in Forestry. EARSeL/ISPRS, Vienna, Austria, 14-15 February 2006, pp. 211-217.

Kohonen, T., Hynninen, J., Kangas, J., Laaksonen, J. 1996. SOM_PAK, The Self-Organizing Map Program Package, Technical Report A31, Helsinki University of Technology, Laboratory of Computer and Information Science, FIN-02150 Espoo, Finland, 27 pages.

Laky, S., Zaletnyik, P., Toth, C. 2010a. Compressing LiDAR waveform data, In: Proc. International LiDAR Mapping Forum, Denver, USA, 3-5 March 2010.

Laky, S., Zaletnyik, P., Toth, C. 2010b: Land classification of wavelet-compressed full-waveform LiDAR data. International Archives of the Photogrammetry Remote Sensing and Spatial Information Sciences (ISSN: 1682-1750) XXXVIII: (3A) 115-119.

Mallet, C., Soergel, U., Bretar, F., 2008. Analysis of full-waveform lidar data for an accurate classification of urban areas. *International Archives of Photogrammetry, Remote Sensing and Spatial Information Sciences* 37 (Part 3A), pp. 85-92.

Mallet, C., Bretar, F., 2009. Full-waveform topographic LiDAR: State-of-the-art, *ISPRS Journal of Photogrammetry and Remote Sensing*, Volume 64, Issue 1, pp. 1-16.

Optech Incorporated, 2005. Airborne Laser Terrain Mapper (ALTM) Waveform Digitizer Manual, Optech Incorporated, Toronto, Ontario, Canada, Document No. 0028443/Rev A.5.

Shan, J., and Toth, C. K., 2009. *Topographic Laser Ranging and Scanning—Principles and Processing*, CRC Press Taylor & Francis, London, 590 pages.

Wagner, W., Ullrich, A., Ducic, V., Melzer, T. and Studnicka, N., 2006. Gaussian decomposition and calibration of a novel small-footprint full-waveform digitising airborne laser scanner. *ISPRS Journal of Photogrammetry & Remote Sensing* 60(2), pp. 100–112.

Zaletnyik, P., Laky, S., Toth, C., 2010. LiDAR waveform classification using Self-Organizing Map, ASPRS, San Diego, CA, 28-30 April 2010.